Journal of Colloid and Interface Science 383 (2012) 124–129

Contents lists available at SciVerse ScienceDirect

Journal of Colloid and Interface Science

www.elsevier.com/locate/jcis

Foam films in the presence of functionalized gold nanoparticles

Janine Emile [a,*], Martinus H.V. Werts [b], Franck Artzner [a], Federico Casanova [a], Olivier Emile [c], Julien R.G. Navarro [b], Florian Meneau [d]

[a] Institut de Physique de Rennes, CNRS UMR 6521, Université de Rennes I, Campus de Beaulieu, 35042 Rennes, France
[b] Laboratoire SATIE, CNRS UMR 8029, Ecole Normale Supérieure de Cachan-Bretagne, Campus de Ker Lann, 35170 Bruz, France
[c] Laboratoire de Physique des Lasers, URU 435, Université de Rennes 1, Campus de Beaulieu, 35042 Rennes, France
[d] Beamline SWING, Synchrotron SOLEIL, 91191 Gif-sur-Yvette, France

ARTICLE INFO

Article history:
Received 14 May 2012
Accepted 16 June 2012
Available online 27 June 2012

Keywords:
Gold nanoparticle
Foam
Film thickness
Small-angle X-ray scattering (SAXS)
Laser interferometry

ABSTRACT

Dry aqueous foams made of anionic surfactant (SDS) and spherical gold nanoparticles are studied by small angle X-ray scattering and by optical techniques. To obtain stable foams, the surfactant concentration is well above the critical micelle concentration. The specular reflectivity signal obtained on a very thin film (thickness 20 nm) shows that functionalized nanoparticles (17 nm typical size) are trapped within the film in the form of a single monolayer. In order to isolate the film behavior, investigations are made on a single film confined in a tube. The film thinning according to the ratio of functionalized nanoparticle and SDS micelles (1:1, 1:10, 1:100) is mainly governed by the structural arrangement of SDS micelles. In thick films, nanoparticles tend to form aggregates that disappear during drainage. In particular self-organization of nanoparticles (with different surface charge) inside the film is not detected.

1. Introduction

The stability of aqueous foams in presence of particles has attracted many industrial applications (food manufacturing, cosmetic formulations, flotation, treatment of nuclear waste, etc.) [1]. The optical and electronic properties of metallic nanoparticles of different size and shape have opened various investigations in photonics [2] and in the life sciences [3]. The integration of nanoparticles into a thin film deposited onto a substrate is relatively well controlled [4]. However, an aqueous foam is an interconnected network which is composed of thin liquid films and large channels (Plateau borders), and particle assembly inside these free liquid surfaces is more delicate. How will nanoparticles be organized at the end of draining? Do they concentrate at the air/liquid interfaces, or inside the films or in Plateau borders?

Surfactant molecules are used in the surface modification and stabilization of gold nanoparticles. However, studies on aqueous foams in presence of gold nanoparticles are scarce. One reason for this is that the concentration of gold nanoparticles in typical colloidal suspensions (~nM) is too low to be conveniently detectable inside thin foam films. Higher nanoparticle concentrations may be obtained by centrifugation of the suspension or evaporation of solvent, but care must be taken not to jeopardize colloidal stability.

As for an anionic surfactant, we chose sodium dodecyl sulfate (SDS, anionic surfactant) for its good foaming properties. To ensure the stability of foams, the solutions are highly concentrated (well above the critical micelle concentration, cmc). At such high surfactant concentrations, a lamellar structure of the micelles (stratification [5]) within the thin liquid film has been proposed to explain the swelling of films set in motion in confined geometries [6]. Spherical gold nanoparticles were functionalized to be introduced in small quantities in the foaming solution. Several more questions then arise. If the nanoparticles are localized in the films, how do they interact with SDS micelles? Will the layer-by-layer assembly of the SDS be preserved? If the nanoparticles are confined in the films, are they organized such that their optical plasmon resonances are coupled resulting in an electromagnetic field enhancement?

In this paper, we report experimental observations that aim to elucidate these questions. For this purpose, we first characterize solutions containing functionalized gold nanoparticles and SDS by UV–visible absorption spectroscopy. Dry foams (liquid fraction below 5%) and single thin films (thickness about 100 nm) are then studied by small angle X-ray scattering (SAXS) and optical interferometry.

2. Solutions of functionalized gold nanoparticles

2.1. Preparation of concentrated suspensions of functionalized gold nanoparticles

Excess citrate-stabilized spherical gold nanoparticles (xCS-AuNP) were prepared according to the well established Turkevich–Frens method [7,8], in which a gold salt ($HAuCl_4$) is reduced

* Corresponding author.
E-mail address: janine.emile@univ-rennes1.fr (J. Emile).

0021-9797/$ - see front matter © 2012 Elsevier Inc. All rights reserved.
http://dx.doi.org/10.1016/j.jcis.2012.06.039

with sodium citrate in aqueous solution. With this procedure, a fairly monodisperse suspension of spherical gold nanoparticles (~15 nm diameter) is obtained. All glassware was cleaned using ultrasound and Ultrasonol 11 solution (Carl Roth, 1:50 in distilled water), followed with thorough rinsing with Milli-Q water. One hundred eighty milliliters of an aqueous solution of chloroauric acid ($HAuCl_4$, 0.3 mM) was placed in a roundbottom flask and brought to a rolling boil with continuous stirring. Subsequently, 10 ml of sodium citrate solution (17 mM in water) was added rapidly. The solution was left stirring for 30 min at 100 °C, and then left to cool down. After cooling at room temperature, the solution was characterized using UV–visible absorption spectroscopy (Ocean Optics USB 4000-VIS–NIR fiber-couple CCD spectrometer with a LS-1 tungsten halogen light source equipped with a BG34 filter), showing a surface plasmon resonance peak at 525 nm. The solution was stored in the dark for at least 24 h. Three procedures were used for the functionalization of the nanoparticles, resulting in positive, negative and neutral surface charge.

To obtain positively charged nanoparticles (labeled Au^+), a solution of 3,6,9,12,37,40,43,46-octaoxa-24,25-dithiaoctatetracontane-1,48-diamine (amino-TEG, 2.4 mg) in 1 ml of ethanol was acidified with 6 µl of 1 M HCl(aq), and subsequently added to 150 ml of the xCS-AuNP suspension [9]. For negatively charged nanoparticles (Au^-), we used 1 ml of an aqueous solution of DL-lipoic acid (2.4 mM) containing 2.4 mM NaOH that was added to 150 ml of xCS-AuNP suspension. Finally, for nanoparticles of neutral charge (Au), 3.5 mg of 3,6,9,12,37,40,43,46-octaoxa-24,25-dithiaoctatetracontane-1,48-diol (TEG) is dissolved in 2 ml of ethanol, and this solution is added to 150 ml of xCS-AuNP suspension. All mixtures were stirred for a period of 15 min and then left overnight.

In order to remove the excess citrate and to increase the nanoparticle concentration from 10^{-9} M to 10^{-6} M, we used three centrifugation steps at 10,000 rpm for 15 min in which the supernatant (90% of the volume) containing free ligands was replaced by additional solution of functionalized nanoparticles, leading to a concentration of particles in each centrifugation step. Finally a washing step with deionized water (for neutral charge nanoparticles, pH = 6.85), NaOH 1 mM (for negatively charged nanoparticles, pH = 11) and HCl 1 mM (for positively charged nanoparticles, pH = 3) was performed. A final nanoparticle concentration of 6×10^{-6} M was estimated using quantitative UV–visible absorbance spectroscopy on diluted samples of the concentrates using literature values of the extinction coefficient [10,11]. No higher concentrations were used in order to avoid problems of unwanted aggregation. To check the stability of functionalized nanoparticles, a drop of 10 µl of each solution was sandwiched between two microscope cover slips and examined by UV–visible spectroscopy (Fig. 1a). For the three types of particles, the plasmon peaks are located at almost the same wavelengths, from 525 nm to 535 nm. The small changes in plasmon resonance reflect changes in local refractive index due to the functionalization and the high optical densities. A nanoparticle core size of approximately 15 nm was confirmed from the ratio of absorbance at the surface plasmon resonance maximum to the absorbance at 450 nm, as described in the literature [10]. This yields an overal core–shell diameter of 17 nm when including the thickness of the ligand shell.

2.2. Mixture of functionalized gold nanoparticles with surfactant

Functionalized gold nanoparticles are mixed with an anionic surfactant, sodium dodecyl sulfate (SDS, ≥99% from Sigma–Aldrich) at a 42 mM concentration, which is far above the critical micellar concentration (cmc 8.2 mM). The mean aggregation number of a SDS micelle is 60 [12]. In the mixture, there are about 100 SDS micelles for 1 gold nanoparticle (100:1). SDS is a well known surfactant and is often used as a reference sample for the study of aqueous foams. We used the same apparatus as in Fig. 1a to characterize the SDS-nanoparticle mixture. The absorption spectrum is not modified for Au and Au^-. However there is a significant shift of the plasmon peak for a drop composed on positively charged nanoparticles Au^+ and SDS (Fig. 1b). One also notices the appearance of a second absorption band at 570 nm. This shoulder is indicative of SDS-mediated interactions between Au^+ nanoparticles, leading to a reduced average distance between nanoparticles, thereby inducing optical interactions that cause a shift of the plasmon band. The existence of two absorption bands suggests that the positively charged particles in SDS are distributed over two types of microenvironment. In one environment they are isolated, in the other they are close and interact. The average length of a SDS molecule is between 1 and 1.5 nm, and the diameter of a micelle is approximately 5 nm. Presumably, negatively charged SDS molecules agglomerate on the surface of Au + nanoparticles, giving an overall core–shell particle diameter between 19 nm and 20 nm. In all cases, no irreversible aggregation occurs, and the mixtures are stable.

In order to confirm these observations, we performed small angle X-ray scattering experiments (SAXS experiments) on the SWING beamline at the SOLEIL synchrotron source. The energy of the beam is 12 keV beam (λ = 1.0344 Å) and it has a 50×300 µm^2 cross-section. The sample to the AVIEX CCD detector distance is fixed at 1.2 m and the resulting scattering vector q ($q = 4\pi \sin(\theta/2)/\lambda$ where θ is the angle between direct beam and scattered beam), ranges from 0.33 to 6.5 nm^{-1}. The acquisition time is 100 ms and solutions sealed inside a 2 mm *diameter* quartz capillaries (10 µl SDS + 10 µl

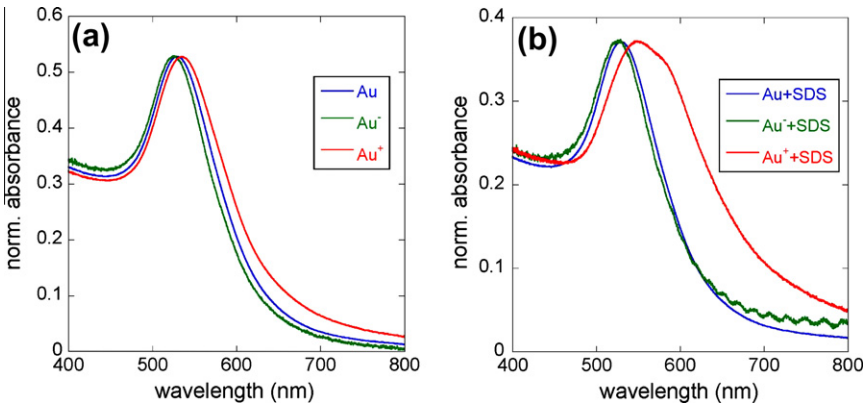

Fig. 1. Normalized UV–visible absorbance spectra for aqueous solutions of functionalized gold nanoparticles at 10^{-6} M (a) and for functionalized gold nanoparticle-SDS mixtures (b).

Au solution) show isotropic scattering. The resulting curves are normalized to take into account the effects related to the detector sensitivity and sample transmission. The q range calibration is made using a silver behenate standard sample. The FIT2D software package is used for data analysis [13].

The system is modeled as monodisperse, noninteracting, hard spheres distributed randomly in solution. The total scattered intensity is then given by the following form factor [14]:

$$I(q) = \left[\frac{3(\sin(qR) - (qR)\cos(qR))}{(qR)^3}\right]^2$$

where R is the hard-sphere radius of the particle.

As a first approximation, the spectra of solutions are refined giving a diameter of 17 ± 0.1 nm for neutral nanoparticles. The model can be improved, providing information about the core and the shell structure of nanoparticles [15]. For the various mixtures without (Fig. 2a) and with SDS (Fig. 2b), the core diameter is always found to be 14.6 ± 0.1 nm in agreement with the 15 nm estimated size from the UV–visible spectroscopic measurement. However, while the overall core–shell diameter of the neutral particle is well defined (17 nm), the refinement gives about 18 ± 1 nm overall diameter for charged (Au^- and Au^+) particles.

3. SDS films in the presence of gold nanoparticles

3.1. Structure of a foam film

To produce the foam, the nanoparticle-SDS solution was beaten stiffly and the foam is introduced in a quartz capillary tube (diameter of 3 mm, 20 µl SDS + 20 µl Au nanoparticle solution) with a syringe. SAXS experiments performed on foams produce 2D scattering patterns which are the sum of an isotropic contribution and an anisotropic scattering, called spikes (Fig. 3a). The isotropic contribution, which has the shape of circular halos, comes mainly from the solution contained in the Plateau border. The other contribution is due to the specular reflection of the parallel X-ray beam on the curved film surface [16]. We have obtained a specular reflectivity profile in the shape of oscillations superimposed with a q^{-4} decay, the so-called Kiessig fringes. Experiments performed on a single film inside an ordered foam (a series of equidistant films in a Kapton tube) give information about the structural organization [17,18]. With a small amount of solution (20 µl for each measurement), it was difficult to stabilize film stack. In addition, the temperature of the experimental room was not controlled and rather high (at least 25 °C). Then the lifetime of the foam is short and the study of a disordered foam with randomly oriented films confined in a capillary tube seemed to be the most effective method to detect the signal related to a spike. Contrary to SDS data [16], the oscillations do not scale with a $\cos^2(qd/2)$ function where d is the film thickness. The data are well fitted with $\sin^2(qd/2)/q^4$ (Fig. 3b). The periodicity of Kiessig fringes leads to an interparticle center-to-center distance d = 17.3 ± 0.2 nm for Au + SDS, Au^- + SDS mixtures and 20.3 ± 0.2 nm for Au^+ + SDS film. The quality of the refinement is governed by the isotropic contribution for which the subtraction of the spectra is difficult. Several scans performed at different places of the nanoparticle-SDS foam lead to similar spikes: all the films have substantially the same thickness. For a film stabilized by SDS, it was possible to distinguish the electron density of SDS layer at the air/liquid interface from that of the solution (aqueous core) layer [16,17]. However, SAXS spectra of foam films containing gold nanoparticles showed that the electron density of gold predominates and the film is simply modeled as a homogenous layer. The functionalized nanoparticles have almost identical diameters. The mixture with SDS surfactant causes a modification of the apparent size of the positively charged nanoparticles, which is likely related to SDS-mediated interactions between Au^+ particles. UV–visible spectra clearly showed this effect. SAXS experiments on foam films indicate that positively charged nanoparticles are influenced by SDS molecules and the effective size increases by 3 nm. The shell is modified by electrostatic interactions between SDS and the capping amino-TEG molecules.

In any case, one can clearly see that whatever the surface modification, functionalized gold nanoparticles are always trapped in films. Despite an estimated concentration of nanoparticles in the film that is higher than in solution, no effect of stratification (self-layering) nor assembly (clustering or aggregates) is observed. Surface tension measurements of films consisting of nanoparticle + SDS mixtures did not show any change in interfacial tension. The air/liquid interface seems to be saturated by SDS molecules and the aqueous core layer is only influenced by gold molecules. However, SAXS data showed that a foam film contains a single monolayer of nanoparticles. The lateral packing of nanoparticles may be periodically arranged, with at least a periodicity above the nanoparticle size (for $q < 0.3\ nm^{-1}$), but no superstructure has been observed.

3.2. Thinning of a vertical free-draining film

Thinning of SDS films in the presence of gold nanoparticles was investigated by home built optical interferometry [6]. The temperature was controlled at 20.0 ± 0.5 °C. We have used low power He–Ne lasers (λ = 543.5 nm and 632.8 nm) to measure the transmitted

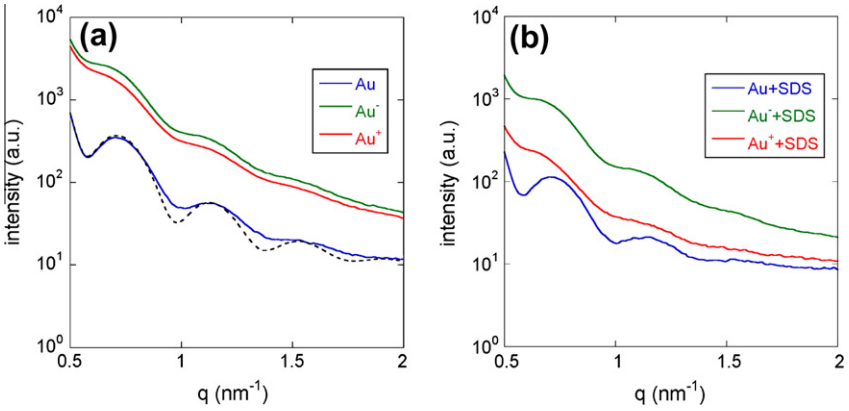

Fig. 2. SAXS spectra for solutions of functionalized gold nanoparticles at 10^{-6} M (a) and for solutions of functionalized gold nanoparticles mixed with SDS (b). The dotted line corresponds to the fit of the data using the parameters given in the text.

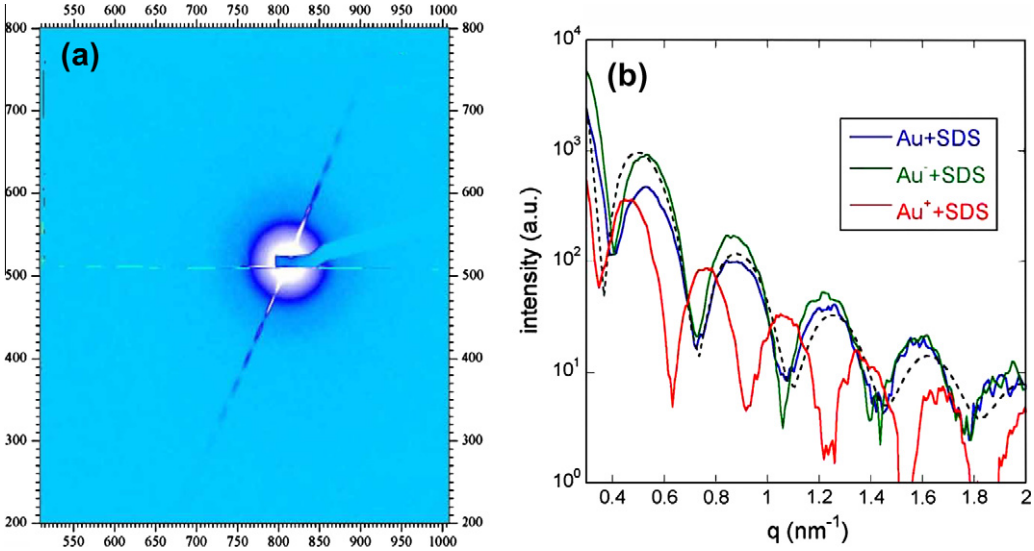

Fig. 3. An example of a SAXS pattern recorded for a Au^+ + SDS foam. The two spikes represent two curved films (a). Integrated intensity along a spike. The dotted line corresponds to the fit of Au + SDS data using the parameters given in the text (b).

signals which cross the film confined in a tube. The intensity transmissivity T is given by:

$$T \approx t^2\left[1 + 2r\cos\left(\frac{4\pi ne}{\lambda}\right)\sin c\left(\frac{2\pi n\Delta e}{\lambda}\right)\right]$$

where r (about 0.02) and t are the reflection and transmission coefficients. One can extract the film thickness e from the positions of minima and maxima of the transmitted intensity. The fringe order is identified by combining the two laser interferences. The amplitude of the transmission curve is modulated by a sinc function which shows that the two air/liquid interfaces of the film are not perfectly parallel. From the expression of intensity transmissivity T, it is also possible to extract the film thickness by comparing its evolution as a function of the two wavelengths. We have checked that the refractive index n has the same value for the film and the corresponding solution.

Using a Hamilton syringe, a small amount of foam solution (10 μl SDS + 10 μl gold solution) was applied to deposit a film inside a circular glass tube (inner diameter 4 mm). The drainage curves (Fig. 4a) are not described by the models used for the study of a film formed by a vertical withdrawal from a liquid bath [19,20]. There are clearly two regimes, one for the short times ($t < 2$ s) with a power law decreases and one for longer time with an exponential decay. The exponential law $\exp(-t/\tau)$ is related to the contribution of surface forces that may be dominant for relatively thick films (100 nm). To ensure the stability of films, the surfactant concentration is high (well above the cmc) and the SDS micelle organization in layers parallel to the film plane (stratification [5]) becomes important. Unlike many studies of surfactant films in a horizontal position (cell with an opening that sucks in liquid), we do not observe a stepwise thinning at a longer time scale [21]. The film breaks as soon as the thickness reaches the critical value of 100 nm. The relaxation time τ is about 4.5 s for SDS and 5.5 s for SDS + nanoparticles. The velocity of thinning depends on the surface forces but also on the bulk viscosity and the surface tension [22]. These film thinning dynamics for other SDS mixture films have also been studied [6], but the precise hydrodynamic analysis for a confined geometry with non-negligible edge effects (direct contact with the meniscus) remains delicate. For the short times, the thinning behavior of the SDS film is a slow $t^{-0.25}$ decrease. However, for the SDS with nanoparticles, the short time draining is divided in two more regimes, the first one with $t < 1$s with a $t^{-0.5}$ law and then a $t^{-0.25}$ decrease as for the SDS alone. The thinning laws for the three functionalized gold particles are very similar. The draining exponents are totally different from those found in the particular case of a large freestanding film [19,20]. Measurements in a tube closed by optical glass windows lead to the same behavior. This shows that the effects of evaporation are negligible. Recently, a fluid dynamic model describing the tear film thinning [23] near the meniscus (in our case this could be the contact between the film and the tube) revealed that the draining exponent is close to −0.5. In this model, the effect of capillarity only is taken into account. When capillarity and gravity are present, the film thickness evolves as $t^{-0.8}$. Although the tube size is greater than the capillary length (3.1 mm), the effect of gravity is only detected for tube sizes of the order of 1 cm. The slight decrease of SDS film ($t^{-0.25}$ decrease) may be attributed to a small difference in surface tension that has not been detected by drop tensiometry measurements which do not allow to probe such dynamics at short times. Adding hydrophilic particles to the SDS film makes no discernible difference to the thinning behavior nor to the film lifetime. Similar results have been obtained for films incorporating silica particles [20].

As it was not possible to increase the gold nanoparticle concentration without aggregation, we modified the ratio of SDS and Au concentrations. The SDS quantity was reduced to 1 μl, then the nanoparticle quantities is increased up to 10 μl and 100 μl, giving about 1 SDS micelle for 10 nanoparticles (1:10) and 1 nanoparticle (1:1) respectively. Drainage curves have the same exponential behavior for different mixtures of functionalized particles (Fig. 4b). The relaxation time τ changes to about 7.5 s for (1:10) and (1:1) quantities. Between 0.4 and 8 s, the nanoparticles are influenced by the organization of SDS micelles. However, increasing the ratio of nanoparticles compared to micelles did not modify significantly the film thinning and no optical absorption effect was detected. This result is particularly surprising since the size of the nanoparticles (typically 17 nm) is relatively large. The film is too thick to highlight the contribution of the surface charge. There is no signature of a lateral assembly of particles that could induce an electromagnetic field enhancement. Whatever the size and shape of the tube containing the film, the rupture thickness remains at 100 nm. The confinement effect related to the meniscus

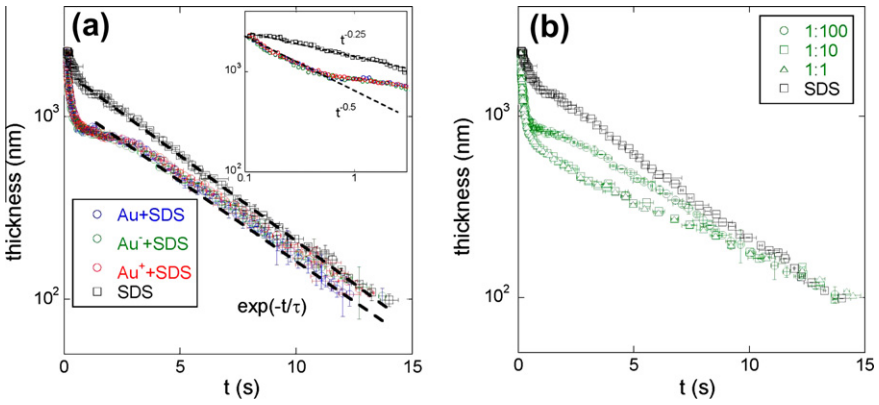

Fig. 4. Drainage of SDS mixture films in a circular tube vs. time (semi-log plot). (a) The ratio of functionalized gold nanoparticle and SDS micelles is 1:100. The dotted lines correspond to the fit of data given in the text. Insert: zoom of data (log–log plot). (b) The ratios of negatively charged gold nanoparticle and SDS micelles are (1:1, 1:10, 1:100).

in direct contact with the tube walls does not allow to evacuate SDS micelle layers and to obtain a very thin film (thickness 20 nm) studied in the case of a dry foam.

In order to gain more insight into the physics behind Fig. 4, we have performed some additional UV–visible absorbance spectroscopy experiments on SDS mixture films, with the ratio (1:100). We have been able to measure the absorption 1 s after the film has formed and to follow the drainage. The thinning curves are very similar to the one obtained with laser interferometry although the resolution is much less. However we can easily follow the plasmon peak resonance vs. the film thickness (Fig. 5). First, the absorption spectra are the same for the various functionalized particles. We have chosen to show the SDS + Au^+ only. After 5 s of drainage, the absorption spectra for the film or for the bulk solution (Fig. 1) are alike although the scale is not exactly the same. This means that the nanoparticles are monodisperse with no aggregation for such thicknesses. At shorter time, between 1 and 5 s, we can see that the plasmon resonance peak strongly varies from $\lambda = 650$ nm to $\lambda = 520$ nm as the thickness varies from 850 nm to 750 nm. This means that in rather thick films, the nanoparticles tend to aggregate and then the aggregation disappears. However, this aggregation is reversible. Unfortunately, we were not able to measure the peak resonance for shorter time and higher thickness in order to investigate the dynamics of the aggregates formation.

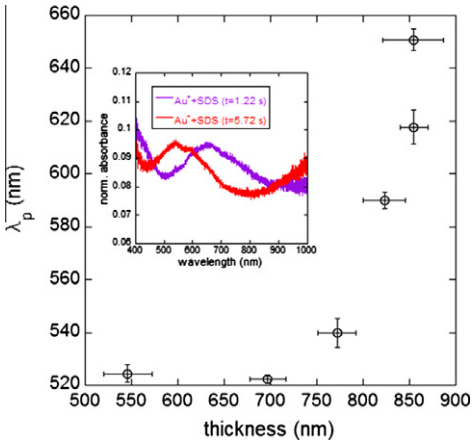

Fig. 5. Position of the surface plasmon resonance peak vs. the thickness of a Au^+ + SDS film. The ratio of functionalized gold nanoparticle and SDS micelles is 1:100. Insert: normalized UV–visible absorbance spectra for two different times during drainage. Note that the absorbance spectra are alike for Au + SDS films and Au^- + SDS films.

As soon as the film started to drain, the SDS and the nanoparticles concentration is much higher than in the bulk solution. Since the film is rather thick, there is little confinement limits and the nanoparticles begin to aggregate. Then it is much easier for the water to flow between the aggregates and the thinning is rather fast. As said previously, capillarity seems to be the leading mechanism. But one cannot exclude the contribution of viscous forces. When the film reaches a thickness of the order of 1 μm, the film interfaces and the confinement start to play a major role. The aggregates undergo interactions and confinements and they collapse between 1 and 5 s. This collapse leads to a variation of the surface tension and then a slower decrease. At the same time a structure begins to appear (stratification) at the interfaces as well as an organization inside the film. For longer time, the film drainage is dominated by the drainage of the SDS film; the nanoparticles do not play any role any more (exponential decrease). In particular our interpretation would mean that the aggregation of nanoparticles is a reversible process when the particles are confined in thin draining films. Of course, it would be very interesting to follow the dynamics of the films in the first second of the drainage.

4. Conclusion

SAXS experiments were performed on a dry foam of SDS in the presence of functionalized gold nanoparticles. The analysis of reflectivity signals unequivocally shows that the nanoparticles are trapped in thin films in the form of a single monolayer. Although the particle concentration inside the film is higher than in solution or in Plateau borders, no self-organization of the particles was detected. Besides, although the nanoparticle concentration is much higher (μM) than the nanomolar concentrations of usual nanoparticle solutions, it remains low compared to the concentration of micelles. The nanoparticle concentration was not increased further to avoid problems of aggregation. The ratio of surfactants and nanoparticles was investigated on a single film confined in a tube of millimeter size. Whatever the quantity of nanoparticles, the thinning dynamics in the presence or absence of nanoparticles remain similar. Since the solution concentrations are well above the cmc, the film drainage is dominated by the stratification of SDS micelles. At short times, some differences related to capillary effects were observed. In thick films, nanoparticles tend to form aggregates that curiously quickly disappear during drainage, meaning that in this case the aggregation process is reversible. Optical spectroscopic measurements show no additional resonances corresponding to the coupling of surface plasmons. The surface chemistry does not seem to be a major parameter in the organization of gold nanoparticles in the

concentration range studied. Even if the drying of a drop of nanoparticle solution on a substrate may provide photonic–plasmonic devices [24], creating photonically active plasmonic nanostructures inside dry foams remains a challenge. The effects of size and shape of metallic nanoparticles on their behavior when confined in foam films is a subject that needs further investigations.

Acknowledgment

Part of this work was supported by the Agence National de la Recherche (ANR-2010-JCJC-1005, Project COMONSENS).

References

[1] R.K. Prudhomme, S.A. Khan, Foams: Theory, Measurement and Applications, Surfactant Science Series 57, Marcel Dekker Inc., New York, 1997.
[2] J.A. Scholl, A.L. Koh, J.A. Dionne, Nature 483 (2012) 421.
[3] G.A. Ozin, A.C. Arsenault, Nanochemistry: A Chemical Approach to Nanomaterials, Royal Society of Chemistry, London, UK, 2005.
[4] Y. Cui, M.T. Björk, J.A. Liddle, C. Sönnichsen, B. Boussert, A.P. Alivisatos, Nano Letters 4 (2004) 1093.
[5] A.D. Nikolov, D.T. Wasan, J. Colloid Interface Sci. 133 (1989) 1.
[6] J. Emile, F. Casanova, G. Loas, O. Emile, Soft Matter 8 (2012) 3223.
[7] G. Frens, Nat. Phys. Sci. 241 (1973) 20.
[8] J. Kimling, M. Maier, B. Okenve, V. Kotaidis, H. Ballot, A. Plech, J. Phys. Chem. B 110 (2006) 15700.
[9] N. Nerambourg, R. Praho, M.H.V. Werts, D. Thomas, M. Blanchard-Desce, Int. J. Nanotechnol. 5 (2008) 722.
[10] W. Haiss, N.T.K. Thanh, J. Aveyard, D.G. Femig, Anal. Chem. 79 (2007) 4215.
[11] M. Loumaigne, R. Praho, D. Nutarelli, M.H.V. Werts, A. Débarre, Phys. Chem. Chem. Phys. 12 (2010) 11004.
[12] N.J. Turro, A. Yekta, J. Am. Chem. Soc. 100 (1978) 5951.
[13] A.P. Hammersley. Scientific software FIT2D; <http://www.ersf.fr/computing/scientific/FIT2D>.
[14] A. Guinier, G. Fournet, Small Angle Scattering of X-rays, John Wiley, New York, 1955.
[15] K. Butter, H. Armin, A. Weidenmann, A.V. Petukhov, G. Vroege, J. Appl. Cryst. 37 (2004) 847.
[16] J. Etrillard, M.A.V. Axelos, I. Cantat, F. Artzner, A. Renault, T. Weiss, R. Delannay, F. Boué, Langmuir 21 (2005) 2229.
[17] E. Terriac, F. Artzner, A. Moréac, C. Meriadec, P. Chasle, J.C. Ameline, J. Ohanna, J. Emile, Langmuir 23 (2007) 12055.
[18] J. Emile, S. Pezennec, A. Renault, E. Robert, F. Artzner, C. Meriadec, A. Faisant, F. Meneau, Soft Matter 7 (2011) 9283.
[19] S. Berg, A.E. Adelizzi, S. Troian, Langmuir 21 (2005) 3867.
[20] S.N. Tan, Y. Yang, R.G. Horn, Langmuir 26 (2010) 63.
[21] K.D. Danov, E.S. Basheva, A.P. Kralchevsky, K.P. Ananthapadmanabhan, A. Lips, Adv. Colloid Interface Sci. 168 (2011) 50.
[22] J.K. Angarska, E.D. Manev, Colloids Surf. A 190 (2001) 117.
[23] R.J. Braun, A.D. Fitt, Math. Med. Biol. 20 (2003) 1.
[24] W.S. Chang, B.A. Willingham, L.S. Slaughter, B.P. Khanal, L. Vigderman, E.R. Zubarev, S. Link, PNAS 108 (2011) 19879.